Toxins **2011**, *3*, 991-1003; doi:10.3390/toxins3080991

OPEN ACCESS

toxins

ISSN 2072-6651
www.mdpi.com/journal/toxins

Article

Molecular Analysis of the Interaction of the Snake Venom Rhodocytin with the Platelet Receptor CLEC-2

Aleksandra A. Watson [1] and Christopher A. O'Callaghan [2,*]

[1] Department of Biochemistry, University of Cambridge/ 80 Tennis Court Road, Cambridge, CB2 1GA, UK; E-Mail: aaw36@cam.ac.uk

[2] Henry Wellcome Building for Molecular Physiology, University of Oxford/ Roosevelt Drive, Oxford, OX3 7BN, UK

* Author to whom correspondence should be addressed; E-Mail: chris.ocallaghan@ndm.ox.ac.uk; Tel.: +44-1865-287789; Fax: +44-1865-287787.

Received: 6 July 2011; in revised from: 21 July 2011 / Accepted: 8 August 2011 / Published: 10 August 2011

Abstract: The Malayan pit viper, *Calloselasma rhodostoma*, produces a potent venom toxin, rhodocytin (aggretin) which causes platelet aggregation. Rhodocytin is a ligand for the receptor CLEC-2 on the surface of platelets. The interaction of these two molecules initiates a signaling pathway which results in platelet activation and aggregation. We have previously solved the crystal structures of CLEC-2 and of rhodocytin, and have proposed models by which tetrameric rhodocytin may interact with either two monomers of CLEC-2, or with one or two copies of dimeric CLEC-2. In the current study we use a range of approaches to analyze the molecular interfaces and dynamics involved in the models of the interaction of rhodocytin with either one or two copies of dimeric CLEC-2, and their implications for clustering of CLEC-2 on the platelet surface.

Keywords: rhodocytin; CLEC-2; platelets; thrombosis

---

1. Introduction

A range of snake toxins have evolved to influence blood clotting and platelet aggregation [1]. Various C-type lectin-like proteins influence platelet aggregation through interactions with receptors on the surface of platelets; a number of these venom proteins are heterodimeric [2,3]. Platelet activation and aggregation can be triggered by various well defined receptors on the surface of

platelets. Under typical physiological conditions, GPIb-V-IX and αIIbβ3 integrin interact with von Willebrand factor when the latter has become attached to extracellular collagen. Collagen itself interacts with the immunoglobulin superfamily receptor GPVI and the integrin α2β1 [4,5]. There is great biomedical interest in the discovery of novel platelet-activating receptors and in this respect the identification of the targets on platelets for snake venom proteins has been an important objective.

The Malayan pit viper *Calloselasma rhodostoma* is a major cause of snakebite morbidity in large parts of Southeast Asia and effects on platelet function are key consequences of envenomation [6]. The pit viper produces a venom protein, rhodocytin (aggretin) which was purified and shown to cause powerful platelet activation and aggregation [7,8]. The molecular cloning and sequence analysis of rhodocytin demonstrated that the two subunits, designated alpha and beta, each have characteristics of the C-type lectin-like family [9]. Rhodocytin has been shown to be a ligand for CLEC-2, a recently identified receptor on the surface of platelets [10]. Binding of rhodocytin to CLEC-2 triggers a potent platelet signaling pathway [10,11]. CLEC-2 contains a single YXXL motif in its cytoplasmic tail. Rhodocytin binding leads to tyrosine phosphorylation in this cytoplasmic tail of CLEC-2, which promotes the binding of spleen tyrosine kinase (Syk), subsequent activation of PLCγ2 and platelet activation and aggregation [10]. CLEC-2 is encoded in a genomic cluster with related C-type lectin-like molecules, some of which have immunological roles, as exemplified by NKG2D [12–17]. CLEC-2 was first identified as a receptor on platelets for rhodocytin and may also play a role in lymphatic development [10,18]. We and others have shown that podoplanin is an endogenous ligand for CLEC-2 [16,19]. Podoplanin is expressed on the luminal aspect of lymphatic endothelial cells and in a range of tissues including kidney, heart, lung and many tumours [20]. The biological importance of CLEC-2 and podoplanin is indicated by observations that genetic knockouts of either molecule are lethal during embryonic development [21–28].

The mechanism whereby rhodocytin triggers platelet aggregation is of great interest because a detailed knowledge of CLEC-2-mediated platelet activation could be of value in understanding and preventing platelet aggregation in thrombotic coronary and cerebral vascular disease, which are major causes of disability and death worldwide. Furthermore, there is a strong need to understand the rhodocytin-CLEC-2 interaction in its own right as snake envenomation affects over 2.5 million humans per year, causing more than 100,000 deaths [29]. We have solved the structure of the C-type lectin-like domain of CLEC-2 and have used mutagenesis to characterise the interaction with rhodocytin [30,31]. The binding affinity of CLEC-2 with rhodocytin and podoplanin has been measured using surface plasmon resonance (Biacore technology) [16,30,32]. We found the affinity of the interaction of rhodocytin with monomeric CLEC-2 to be 1.01 ± 0.20 μM, as compared with 24.5 ± 3.7 μM and 4.1 ± 0.2 μM for the interactions of podoplanin with monomeric and dimeric CLEC-2 respectively [16,30,32].

To further explore the association between CLEC-2 and rhodocytin, we have also solved the crystal structure of rhodocytin, and discovered that it assembles as a non-disulfide linked $(\alpha\beta)_2$ tetramer [33]. Rhodocytin is the first snake venom or other C-type lectin-like protein reported to adopt this configuration. We proposed that the rhodocytin tetramer might induce clustering of CLEC-2 molecules on the platelet surface and that this could play a key role in triggering signaling to platelet activation. We have previously generated three models of the rhodocytin-CLEC-2 interaction, whereby tetrameric rhodocytin may promote clustering of CLEC-2 by interacting with two copies of monomeric CLEC-2,

one copy of dimeric CLEC-2, or two copies of dimeric CLEC-2. We have since used a range of cellular, biochemical and biophysical techniques to demonstrate that CLEC-2 exists as a non-disulfide-linked homodimer [32]. Although Syk generally interacts with two YXXL motifs on a single polypeptide chain, there is evidence to indicate that it can interact with two YXXL motifs, each from a different CLEC-2 chain, consistent with CLEC-2 functioning in a dimeric manner in its interaction with Syk [34]. These observations preclude the first of our original models of the rhodocytin-CLEC-2 interaction, wherein two copies of monomeric CLEC-2 bind to tetrameric rhodocytin. In the current study, we analyse and discuss the interactions involved in the two other models of the interaction, where rhodocytin may bind either one or two copies of dimeric CLEC-2, and discuss the implications for clustering of CLEC-2 on the platelet surface.

2. Materials and Methods

2.1. Protein Interfaces, Surfaces and Assemblies

Algorithms implemented by PISA (Protein interfaces, surfaces and assemblies version 1.2) were used to explore the macromolecular protein interfaces of the model complexes of rhodocytin plus either one, or two copies of model dimeric CLEC-2 [35]. These models were generated as previously reported [33]. These calculations included the structural and chemical properties of macromolecular surfaces and interfaces, the accessible/buried surface area, the free energy of dissociation, and the presence or absence of salt bridges and disulfide bonds. The protein database archive (PDB) was searched for particular interfaces formed by structural homologs, and the PISA database was explored to compare results for multimeric state, symmetry number, space group, accessible/buried surface area, free energy of dissociation, presence/absence of salt bridges and disulfide bonds, homomeric type, and ligands. Structures, interfaces and assemblies were visualised for analysis using Rastop and Jmol (an open-source Java viewer for chemical structures in 3D. http://www.jmol.org/).

2.2. Molecular Dynamics

The potential modes of motion of the different models of the rhodocytin-CLEC-2 complex were examined and analysed using the Dynamite package [36]. From the input three dimensional structure, an ensemble of structures was generated, and subsequently analysed to predict which elements move together and the relevant vectors of these motions. The ensemble was generated using Concoord, and the analysis was performed using Gromacs. In essence, Concoord is used to identify all interatomic interactions in the structure which is input [37]. The likely strength of these interactions is analysed and so the potential freedom of the interacting species is modeled to within appropriate bounds. Following this, new variant structures are established that fulfill the limitations of these modeled bounds. These dynamic analyses were represented graphically using Visual Molecular Dynamics (VMD) [38].

3. Results and Discussion

3.1. The Interaction Surfaces of the Rhodocytin-CLEC-2 Interaction

There are two alpha and two beta subunits of rhodocytin per tetrameric unit. The most basic model of the interaction of rhodocytin with CLEC-2 is that in which one molecule of dimeric CLEC-2 is complexed with one molecule of rhodocytin, the rhodocytin being in the form of the non-disulfide linked $(\alpha\beta)_2$ tetramer that was identified by crystallography [33]. In this complex, there are two hydrogen bonds and one salt bridge involved in the interaction between dimeric CLEC-2 and one beta subunit of rhodocytin (Table 1). However, in this model, the other beta subunit of the tetramer does not bind to the CLEC-2 dimer (Table 1). In addition to the interactions with the beta subunit of rhodocytin, dimeric CLEC-2 interacts with one alpha subunit of rhodocytin through five hydrogen bonds and three salt bridges (Table 1). In contrast to the beta subunits, where only one interacts with CLEC-2, this second alpha subunit does interact with the CLEC-2 dimer in this model, but does not form any ionic bonds with it (Table 1). It is likely that this interaction with the second alpha subunit is mediated by van der Waals forces.

The more complex model of the rhodocytin-CLEC-2 interaction involves two copies of dimeric CLEC-2 bound to one molecule of the non-disulfide linked $(\alpha\beta)_2$ tetrameric form of rhodocytin. It is important to note that this model is distinct from that described above, and has been generated independently in a way that has not been influenced by the first model. In this complex, four hydrogen bonds and one salt bridge are involved in the interaction between each molecule of dimeric CLEC-2 and each rhodocytin beta subunit (Table 2). In addition, the interaction between each alpha subunit of rhodocytin and each molecule of dimeric CLEC-2 involves a further two hydrogen bonds and one salt bridge (Table 2). Clearly, this model in which two CLEC-2 dimers associate with tetrameric rhodocytin involves more numerous and favourable ionic interactions and hydrogen bonds (a total of sixteen, as opposed to eleven interactions per tetramer of rhodocytin) in addition to van der Waals contacts and would therefore be a more likely model (Figure 1). Interestingly, residue K150 of CLEC-2, which we identified as being important for its interaction with rhodocytin using mutagenesis and surface plasmon resonance, is also involved in the interface in this model of the complex [30].

There are 246 bound water molecules present in the crystal structure of monomeric CLEC-2 and 45 water molecules present in the crystal structure of rhodocytin. Therefore, upon dimerization of CLEC-2 and complexing of this dimeric CLEC-2 with tetrameric rhodocytin, there will be considerable liberation of the water molecules which solvate the unbound molecules. In our model where one copy of dimeric CLEC-2 binds tetrameric rhodocytin, the alpha subunits and the one beta subunit involved in the complex experience gains in the free energy of solvation of 1.5, 2.5 and 0.2 kcal/mol respectively (total 4.2 kcal/mol). However, in our more complex model in which two CLEC-2 dimers bind to one tetramer of rhodocytin, the solvation energy gains for each CLEC-2 dimer interaction are 0.2 and 0.6 kcal/mol for the alpha subunits, and 2.2 and 0.7 kcal for the two beta subunits (total 7.4 kcal/mol). There is, therefore, a more appreciable gain in the free energy of solvation upon formation of the complex of two CLEC-2 dimers rather than one with tetrameric rhodocytin, which again indicates that this is a more plausible model.

Table 1. Contact information and interfacing residues involved in the model interaction of one copy of dimeric CLEC-2 with tetrameric rhodocytin. Key: H = residues making hydrogen bonds, S = residues making a salt bridge, ASA = accessible surface area (Å²), BSA = buried surface area (Å²), ΔiG = solvation energy effect (kcal/mol), |||| = buried area percentage, one bar per 10%.

	Rhodocytin alpha chain #1		CLEC-2	
Number of atoms				
interface	17	(1.5%)	18	(0.9%)
surface	715	(63.8%)	1129	(54.1%)
total	1121	(100.0%)	2085	(100.0%)
Number of residues				
interface	8	(6.0%)	5	(2.1%)
surface	123	(92.5%)	222	(91.7%)
total	133	(100.0%)	242	(100.0%)
Solvent-accessible area, Å²				
interface	150.2	(1.8%)	164.3	(1.3%)
total	8404.1	(100.0%)	12294.5	(100.0%)
Solvation energy, kcal/mol				
isolated structure	−94.6	(100.0%)	−222.4	(100.0%)
gain at complexation	−1.5	(1.5%)	−0.1	(0.0%)
average gain	−0.6	(0.6%)	−0.1	(0.0%)
P-value	0.229		0.543	

Rhodocytin alpha chain #1	Ionic bond	ASA	BSA	ΔiG
GLN 23		121.22	3.01 |	−0.01
THR 25		22.63	0.37 |	−0.00
GLU 28		75.89	9.81 ||	−0.17
ASP 100		142.06	7.22 |	−0.12
HIS 102		113.98	18.44 ||	−0.05
GLU 124		74.46	21.29 |||	0.20
GLN 125		78.37	23.20 |||	−0.00
MET 126		86.41	66.86 |||||||	1.61

CLEC-2	Ionic bond	ASA	BSA	ΔiG
ASP 188		138.86	6.93 |	−0.03
LYS 190		135.33	86.75 |||||||	−0.38
ASN 192		110.81	36.12 ||||	−0.02
PHE 207		59.76	31.74 |||||	0.51
ASN 210		66.39	2.72 |	0.00

	Rhodocytin alpha chain #2		CLEC-2	
Number of atoms				
interface	52	(4.6%)	68	(3.3%)
surface	713	(63.6%)	1129	(54.1%)
total	1121	(100.0%)	2085	(100.0%)
Number of residues				
interface	15	(11.3%)	22	(9.1%)
surface	123	(92.5%)	222	(91.7%)
total	133	(100.0%)	242	(100.0%)
Solvent-accessible area, Å²				
interface	587.3	(7.0%)	537.5	(4.4%)
total	8416.9	(100.0%)	12294.5	(100.0%)
Solvation energy, kcal/mol				
isolated structure	−94.8	(100.0%)	−222.4	(100.0%)
gain at complexation	−2.5	(2.6%)	2.8	(−1.3%)
average gain	−1.7	(1.8%)	−0.3	(0.2%)
P-value	0.373		0.895	

Rhodocytin alpha chain #2	Ionic bond	ASA	BSA	ΔiG
GLN 23	H	120.27	74.93 ||||||	−0.33
GLU 28		81.78	1.71 |	−0.02
ASP 66		125.72	28.70 |||	0.14
GLU 67		18.44	1.15 |	0.02
ASP 68	HS	85.58	75.58 ||||||||	−0.77
TYR 69		37.03	3.53 |	0.05
ASP 100	HS	142.47	47.16 ||||	−0.02
HIS 102		113.24	7.72 |	−0.29
LYS 111	H	91.53	63.63 ||||||	−0.03
LEU 112		155.55	127.31 ||||||||	1.55
GLY 114		47.05	5.54 ||	0.06
GLU 124		72.61	2.09 |	−0.02
GLN 125		72.41	55.90 |||||||	0.02
MET 126		94.24	79.53 ||||||||	1.92
HIS 127		19.00	12.81 ||||||	0.20

CLEC-2	Ionic bond	ASA	BSA	ΔiG
ASN 120		97.19	3.68 |	0.00
LYS 150		76.82	4.77 |	0.03
HIS 154	HS	42.91	12.38 |||	−0.24
LEU 155		46.25	4.86 ||	0.08
ILE 156		42.53	22.40 |||||	0.02
GLU 187		57.90	1.47 |	−0.02
TYR 197		38.02	10.89 |||	−0.11
HIS 199		51.26	47.31 ||||||||	−0.90
ASN 200		79.07	56.83 |||||||	−0.09
LYS 202	H	95.17	47.42 |||||	−0.42
HIS 204		43.12	29.08 ||||||	0.07
GLU 209		125.40	0.61 |	−0.01
ASN 210		66.39	8.19 ||	0.01
LYS 211	HS	122.09	33.70 |||	−0.14
HIS 212		32.27	7.81 |||	0.13
ARG 118	HS	100.93	45.82 |||||	−0.76
ASN 120		102.89	66.75 ||||||	0.09
LEU 155		42.73	22.76 |||||	0.36
ILE 156		44.58	18.67 |||||	0.05
LYS 211		116.36	11.88 ||	−0.04
HIS 212		33.89	19.92 |||||	−0.78
TYR 213	H	60.85	60.26 ||||||||	−0.15

	Rhodocytin beta chain #1		CLEC-2	
Number of atoms				
interface	18	(1.7%)	12	(0.6%)
surface	638	(61.6%)	1129	(54.1%)
total	1035	(100.0%)	2085	(100.0%)
Number of residues				
interface	8	(6.5%)	6	(2.5%)
surface	112	(91.1%)	222	(91.7%)
total	123	(100.0%)	242	(100.0%)
Solvent-accessible area, Å²				
interface	130.6	(1.6%)	154.2	(1.3%)
total	7933.1	(100.0%)	12294.5	(100.0%)
Solvation energy, kcal/mol				
isolated structure	−107.9	(100.0%)	−222.4	(100.0%)
gain at complexation	−0.2	(0.2%)	1.7	(−0.7%)
average gain	−0.5	(0.5%)	−0.1	(0.0%)
P-value	0.609		0.935	

Rhodocytin beta chain	Ionic bond	ASA	BSA	ΔiG
ASN 22		69.56	20.99 ||||	−0.00
ARG 100		96.44	12.38 ||	−0.16
GLU 105	HS	81.89	22.63 |||	−0.07
LEU 107		47.78	10.71 |||	0.17
ASP 110		76.19	0.24 |	−0.00
SER 112	H	79.62	35.64 |||||	−0.17
SER 113		39.33	5.85 ||	0.09
THR 114		83.92	22.18 |||	0.35

CLEC-2	Ionic bond	ASA	BSA	ΔiG
ASN 120		97.19	23.61 |||	0.02
LYS 211	HS	122.09	27.30 |||	−1.01
GLU 187		54.63	19.30 ||||	−0.30
ASP 188		135.67	6.75 |	−0.08
LYS 202	H	90.50	65.54 |||||||	−0.48
HIS 204		48.24	11.72 |||	0.19

Table 2. Contact information and interfacing residues involved in the model interaction of two copies of dimeric CLEC-2 with tetrameric rhodocytin. Key: H = residues making hydrogen bonds, S = residues making a salt bridge, ASA = accessible surface area (Å), BSA = buried surface area (Å²), ΔiG = solvation energy effect (kcal/mol), |||| = buried area percentage, one bar per 10 %.

	Rhodocytin alpha chain #1		CLEC-2	
Number of atoms				
interface	19	(1.8%)	14	(0.7%)
surface	698	(64.7%)	1091	(53.8%)
total	1079	(100.0%)	2029	(100.0%)
Number of residues				
interface	11	(8.3%)	8	(3.3%)
surface	123	(93.2%)	219	(90.9%)
total	132	(100.0%)	241	(100.0%)
Solvent-accessible area, Å^2				
interface	86.1	(1.1%)	95.7	(0.8%)
total	8163.2	(100.0%)	11998.6	(100.0%)
Solvation energy, kcal/mol				
isolated structure	−102.9	(100.0%)	−240.7	(100.0%)
gain at complexation	−0.2	(0.2%)	0.7	(−0.3%)
average gain	−0.5	(0.4%)	0.0	(−0.0%)
P-value	0.590		0.737	

Rhodocytin alpha chain #1	Ionic bond	ASA	BSA	ΔiG
GLN 23		108.13	1.22 |	−0.02
GLU 67		14.14	0.49 |	−0.01
ASP 68	HS	81.41	35.61 |||||	−0.14
TYR 69		36.42	7.12 ||	0.11
ASP 100		141.21	0.50 |	0.01
LEU 112		147.96	15.33 ||	0.06
THR 113		45.14	4.02 |	0.04
TYR 121		35.14	2.70 |	−0.03
TYR 122		69.39	2.21 |	−0.03
GLN 125		64.01	1.17 |	−0.01
HIS 127		18.53	15.77 ||||||||	0.25

CLEC-2	Ionic bond	ASA	BSA	ΔiG
ARG 143	HS	161.22	52.59 ||||	−0.74
ASN 144		82.06	1.75 |	−0.02
GLU 147		55.82	16.53 |||	−0.14
LYS 150		79.33	0.26 |	−0.01
GLU 184		139.38	1.23 |	−0.01
ASP 188		139.39	0.49 |	−0.01
LYS 202		96.42	2.31 |	0.03
HIS 119		80.14	20.51 |||	0.23

	Rhodocytin alpha chain #2		CLEC-2	
Number of atoms				
interface	51	(4.7%)	53	(2.6%)
surface	699	(64.8%)	1085	(53.5%)
total	1079	(100.0%)	2029	(100.0%)
Number of residues				
interface	14	(10.6%)	19	(7.9%)
surface	123	(93.2%)	220	(91.3%)
total	132	(100.0%)	241	(100.0%)
Solvent-accessible area, Å^2				
interface	562.3	(6.9%)	459.1	(3.8%)
total	8165.3	(100.0%)	12027.2	(100.0%)
Solvation energy, kcal/mol				
isolated structure	−103.6	(100.0%)	−240.8	(100.0%)
gain at complexation	−0.6	(0.6%)	−0.5	(0.2%)
average gain	−1.2	(1.2%)	0.2	(−0.1%)
P-value	0.638		0.406	

Rhodocytin alpha chain #2	Ionic bond	ASA	BSA	ΔiG
ASP 66	HS	130.36	79.17 ||||||	−0.03
ASP 68		81.94	71.50 ||||||||	−0.55
TYR 69		36.31	27.26 |||||||	−0.04
LYS 104		93.33	36.30 ||||	−1.07
GLU 110		23.39	6.91 |||	−0.06
LYS 111		93.46	64.69 ||||||	0.62
LEU 112		147.63	143.96 |||||||||	1.57
THR 113		44.93	9.95 |||	0.07
GLY 114		46.88	2.48 |	−0.03
LYS 117		141.41	26.11 ||	0.42
TYR 121		35.30	25.21 |||||||	−0.13
TYR 122		68.95	35.37 |||||	0.07
GLN 125	H	63.99	30.94 |||||	−0.33
MET 126		101.87	2.47 |	0.10

CLEC-2	Ionic bond	ASA	BSA	ΔiG
ASN 120		78.74	8.01 ||	−0.09
HIS 154		47.02	20.87 |||||	−0.20
LEU 155		35.70	29.71 ||||||||	0.48
ILE 156		53.72	53.60 |||||||||	0.73
GLU 187		56.68	10.36 ||	−0.12
TYR 197		32.06	19.76 ||||||	−0.19
HIS 199		50.16	48.10 |||||||||	0.23
ASN 200		79.01	17.04 |||	−0.12
LYS 202	HS	98.88	29.20 |||	−0.57
HIS 204		50.56	38.80 |||||||	0.13
PHE 207		75.23	17.03 |||	0.27
GLU 209		126.27	3.80 |	−0.04
ASN 210	H	58.58	45.69 ||||||||	−0.24
LYS 211		115.90	44.00 ||||	−0.06
HIS 212		35.13	27.56 |||||||	0.15
TYR 213		66.22	13.26 |||	0.21
HIS 154		29.40	6.68 |||	−0.08
HIS 199		52.25	16.26 ||||	0.15
ASN 200		73.94	9.33 ||	−0.16

	Rhodocytin beta chain #1		CLEC-2	
Number of atoms				
interface	44	(4.4%)	45	(2.2%)
surface	626	(62.2%)	1085	(53.5%)
total	1006	(100.0%)	2029	(100.0%)
Number of residues				
interface	15	(12.3%)	16	(6.6%)
surface	111	(91.0%)	220	(91.3%)
total	122	(100.0%)	241	(100.0%)
Solvent-accessible area, Å^2				
interface	390.7	(5.0%)	411.1	(3.4%)
total	7813.8	(100.0%)	12027.2	(100.0%)
Solvation energy, kcal/mol				
isolated structure	−111.3	(100.0%)	−240.8	(100.0%)
gain at complexation	−2.2	(1.9%)	1.8	(−0.7%)
average gain	−0.8	(0.8%)	0.1	(−0.1%)
P-value	0.290		0.799	

Rhodocytin beta chain #1	Ionic bond	ASA	BSA	ΔiG
PRO 20		80.18	7.37 |	0.12
LEU 63		30.42	8.55 |||	0.14
GLN 91		119.63	31.40 |||	−0.47
GLU 92		158.11	54.64 ||||	−0.10
GLN 93		105.23	12.72 ||	0.20
SER 94		30.87	0.24 |	−0.00
GLU 95	S	50.04	24.82 |||||	−0.19
ARG 100		98.07	3.35 |	−0.12
ASN 108	H	74.11	14.85 |||	−0.22
MET 109		53.08	44.57 ||||||||	1.42
ASP 110	H	75.54	64.97 ||||||||	0.15
SER 112		83.61	44.24 ||||||	−0.13
SER 113		37.64	35.97 ||||||||	0.58
THR 114		82.96	38.52 |||||	0.60
CYS 115		10.14	4.47 |||||	0.18

CLEC-2	Ionic bond	ASA	BSA	ΔiG
ARG 118		61.27	6.80 ||	−0.01
HIS 119		78.21	35.49 |||||	−0.68
ASN 120	H	78.74	50.66 |||||||	−0.21
LEU 121		32.06	29.72 |||||||||	0.48
THR 122		29.65	12.79 |||||	0.20
GLU 124		105.69	3.56 |	0.06
GLU 125		90.53	64.70 ||||||||	−0.51
GLN 128		94.77	6.26 |	0.10
TYR 129		54.87	16.90 ||||	0.27
ASP 132		99.68	21.00 |||	−0.17
LEU 155		35.70	5.35 ||	0.09
LYS 211	HS	115.90	71.91 |||||||	−1.17
TYR 213		66.22	33.75 ||||||	−0.29
LYS 150		75.88	2.85 |	0.05
HIS 154		29.40	1.51 |	0.02
ASN 200		73.94	47.86 |||||||	0.02

Figure 1. Representation of an interface between CLEC-2 (white) and a beta subunit (pink) of the rhodocytin tetramer. Sidechains of interacting residues (N120 and K211 on CLEC-2, and E95 and D110 on the beta subunit of rhodocytin) are represented as balls and sticks. Predicted hydrogen bonds are represented by broken dotted blue lines.

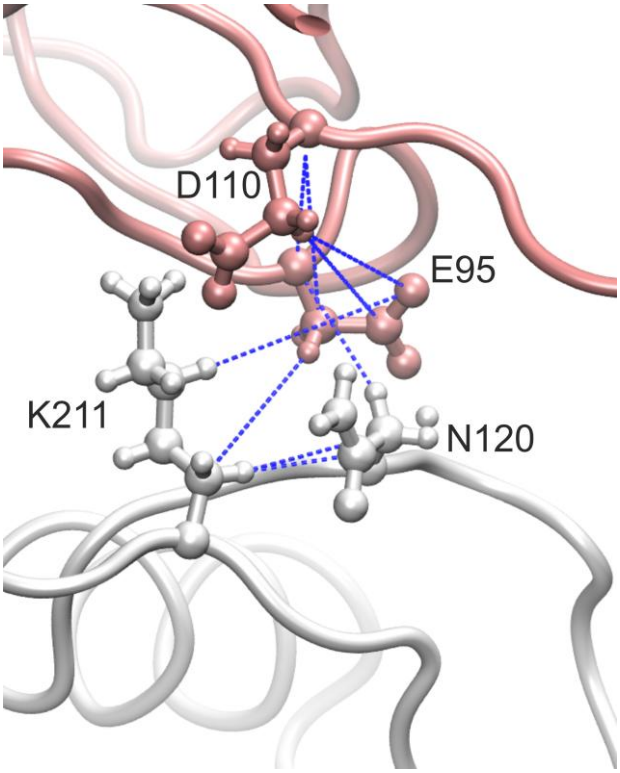

3.2. Dynamic Flexibility of the Rhodocytin-CLEC-2 Complexes

Molecular dynamics analyses were undertaken to investigate the potential flexibility of the two possible rhodocytin-CLEC-2 interaction models (Figures 2, 3). With only a single dimer of CLEC-2 interacting with tetrameric rhodocytin, the predicted motions are dominated by the alpha and beta subunits of rhodocytin and the motions of CLEC-2 appear to play a relatively minor part in the overall flexibility of the complex (Figure 2). Interestingly, in the model with two copies of dimeric CLEC-2 bound to rhodocytin, a much greater contribution is made by the CLEC-2 dimers, and the beta subunits of rhodocytin, to the global flexibility of the complex (Figure 3). In the molecular dynamics simulations for this model, the CLEC-2 dimers appear to wrap around the grooves presented on rhodocytin, and the beta subunits move in a complementary fashion so as to maximise the exposure and accessibility of the two binding grooves to CLEC-2 (Figure 3). Thus, in this interaction mode with two CLEC-2 molecules, the alpha subunits of rhodocytin make a relatively more minor contribution to the possible dynamic motions of the complex (Figure 3).

Figure 2. Dynamic analyses of a model of the interaction of dimeric CLEC-2 (white) with tetrameric rhodocytin. The rhodocytin α- and β-chains are coloured yellow and pink, respectively. The porcupine plots represent the principal mode of conformational variability of the Cα atoms calculated from a CONCOORD ensemble using the model of the rhodocytin-CLEC-2 interaction based on the crystal structure of rhodocytin, and a model of the dimeric structure of CLEC-2. Blue cones represent the direction of each motion; the length of the cone is proportional to the amplitude of the motion. The top image represents a 90 ° counter-clockwise rotation of the central image about the X-axis. The bottom image represents a 90 °clockwise rotation of the top image about the Y-axis.

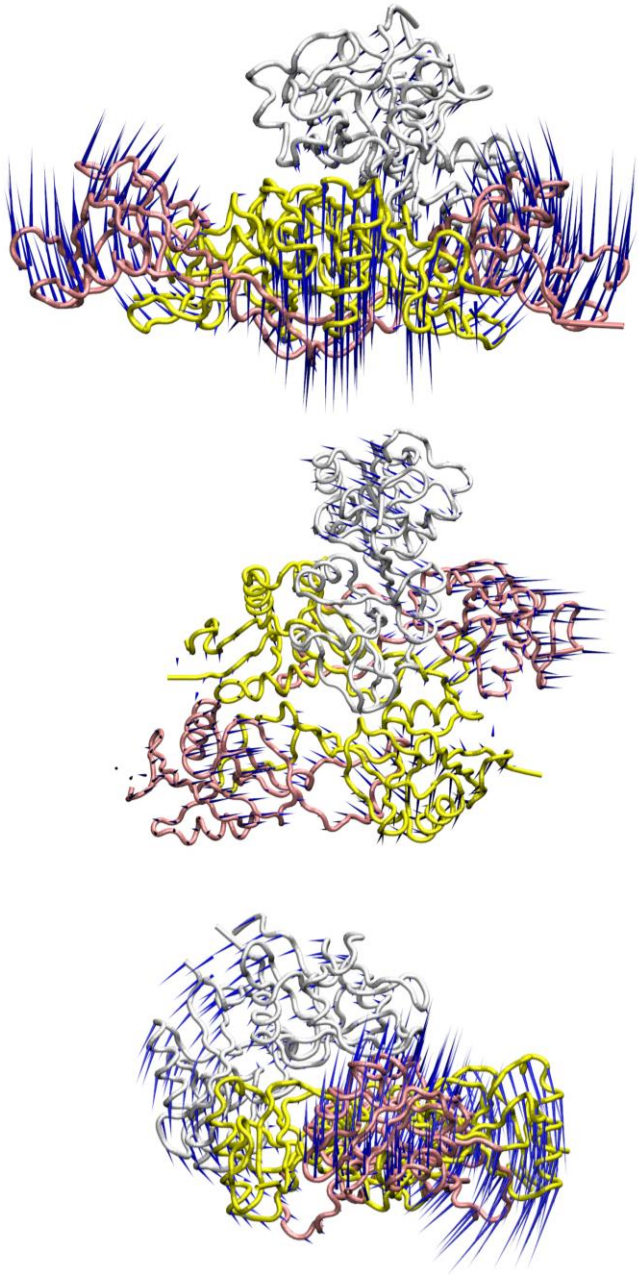

Figure 3. Dynamic analyses of a model of the interaction of two copies of dimeric CLEC-2 (white) with tetrameric rhodocytin. The rhodocytin α- and β-chains are coloured yellow and pink, respectively. The porcupine plots represent the principal mode of conformational variability of the Cα atoms calculated from a CONCOORD ensemble using the model of the rhodocytin-CLEC-2 interaction based on the crystal structure of rhodocytin, and a model of the dimeric structure of CLEC-2. Blue cones represent the direction of each motion; the length of the cone is proportional to the amplitude of the motion. The top image represents a 90 ° counter-clockwise rotation of the central image about the X-axis. The bottom image represents a 90 ° clockwise rotation of the top image about the Y-axis.

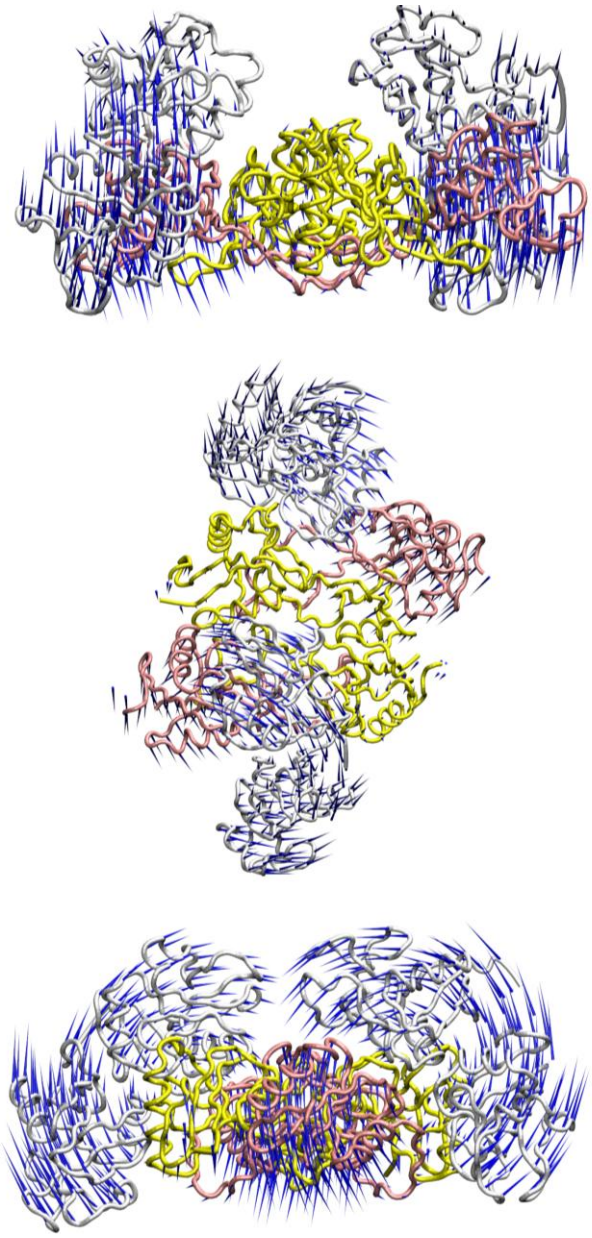

4. Conclusions

We have previously solved the crystal structures of both rhodocytin and CLEC-2, but there is no crystallographic structure of the rhodocytin-CLEC-2 complex. Using three dimensional structures of

both rhodocytin and CLEC-2, we have generated models of the likely modes of interaction of the venom protein and its receptor on platelets and have investigated and analysed the computational models of the interaction which we have generated [30,32,33]. Using a set of analytical algorithms and approaches, we have assessed the properties of the interfacing surfaces and the contribution made to the interaction by specific intermolecular contacts, including salt bridges and hydrogen bonds. In addition to this, we have evaluated the potential flexibility of these model complexes. The model wherein two molecules of CLEC-2 associate with tetrameric rhodocytin provides a more plausible model in terms of the composite effects related to the number of interfacing residues, the nature of their interactions and the predicted solvation energy effects. Further, it is of potential significance that the predicted dynamic motions of this complex are suggestive of a mechanism whereby this interaction might cluster the receptors on the platelet surface, which could have implications for signaling. Overall, the work presented indicates that a plausible mode of binding is that of one non-disulfide linked $(\alpha\beta)_2$ tetramer of rhodocytin with two dimers of CLEC-2. This analysis will be of value in the development of further studies to characterise the interaction further with a view to developing therapeutic approaches to disrupt the rhodocytin-CLEC-2 interaction on the platelet surface.

Acknowledgments

This work was funded by the British Heart Foundation. AAW is a Sir Henry Wellcome Postdoctoral Fellow. We are grateful to Steve Watson for helpful discussions.

Conflict of Interest

The authors declare no conflict of interest.

References

1. Pirkle, H.; Markland, F.S., Jr. *Hemostasis and Animal Venoms*; Dekker: New York, NY, USA, 1987.
2. Clemetson, K.J.; Lu, Q.; Clemetson, J.M. Snake venom proteins affecting platelets and their applications to anti-thrombotic research. *Curr. Pharm. Des.* **2007**, *13*, 2887–2892.
3. Clemetson, K.J.; Lu, Q.; Clemetson, J.M. Snake C-type lectin-like proteins and platelet receptors. *Pathophysiol. Haemost. Thromb.* **2005**, *34*, 150–155.
4. Ruggeri, Z.M. Platelets in atherothrombosis. *Nat. Med.* **2002**, *8*, 1227–1234.
5. Lusis, A.J. Atherosclerosis. *Nature* **2000**, *407*, 233–241.
6. Ho, M.; Warrell, D.A.; Looareesuwan, S.; Phillips, R.E.; Chanthavanich, P.; Karbwang, J.; Supanaranond, W.; Viravan, C.; Hutton, R.A.; Vejcho, S. Clinical significance of venom antigen levels in patients envenomed by the malayan pit viper (*Calloselasma rhodostoma*). *Am. J. Trop. Med. Hyg.* **1986**, *35*, 579–587.
7. Huang, T.F.; Liu, C.Z.; Yang, S.H. Aggretin, a novel platelet-aggregation inducer from snake (Calloselasma rhodostoma) venom, activates phospholipase c by acting as a glycoprotein ia/iia agonist. *Biochem. J.* **1995**, *309*, 1021–1027.

8. Shin, Y.; Morita, T. Rhodocytin, a functional novel platelet agonist belonging to the heterodimeric c-type lectin family, induces platelet aggregation independently of glycoprotein ib. *Biochem. Biophys. Res. Commun.* **1998**, *245*, 741–745.
9. Chung, C.H.; Au, L.C.; Huang, T.F. Molecular cloning and sequence analysis of aggretin, a collagen-like platelet aggregation inducer. *Biochem. Biophys. Res. Commun.* **1999**, *263*, 723–727.
10. Suzuki-Inoue, K.; Fuller, G.L.; Garcia, A.; Eble, J.A.; Pohlmann, S.; Inoue, O.; Gartner, T.K.; Hughan, S.C.; Pearce, A.C.; Laing, G.D.; *et al.* A novel Syk-dependent mechanism of platelet activation by the C-type lectin receptor CLEC-2. *Blood* **2006**, *107*, 542–549.
11. Fuller, G.L.; Williams, J.A.; Tomlinson, M.G.; Eble, J.A.; Hanna, S.L.; Pohlmann, S.; Suzuki-Inoue, K.; Ozaki, Y.; Watson, S.P.; Pearce, A.C. The C-type lectin receptors CLEC-2 and Dectin-1, but not DC-SIGN, signal via a novel YXXL-dependent signaling cascade. *J. Biol. Chem.* **2007**, *282*, 12397–12409.
12. O'Callaghan, C.A. Thrombomodulation via CLEC-2 targeting. *Curr. Opin. Pharmacol.* **2009**, *9*, 90–95.
13. O'Callaghan, C.A.; Tormo, J.; Willcox, B.E.; Braud, V.M.; Jakobsen, B.K.; Stuart, D.I.; McMichael, A.J.; Bell, J.I.; Jones, E.Y. Structural features impose tight peptide binding specificity in the non-classical MHC molecule HLA-E. *Mol. Cell* **1998**, *1*, 531–541.
14. Braud, V.; Allan, D.S.J.; O'Callaghan, C.A.; Ogg, G.S.; Lazetic, S.; Young, N.T.; Bell, J.I.; Phillips, J.H.; Lanier, L.L.; McMichael, A.J. HLA-E binds to natural killer cell receptors CD94/NKG2A, B and C. *Nature* **1998**, *391*, 795–799.
15. O'Callaghan, C.A.; Cerwenka, A.; Willcox, B.E.; Lanier, L.L.; Bjorkman, P.J. Molecular competition for NKG2D: H60 and RAE1 compete unequally for NKG2D with dominance of H60. *Immunity* **2001**, *15*, 201–211.
16. Christou, C.M.; Pearce, A.C.; Watson, A.A.; Mistry, A.R.; Pollitt, A.Y.; Fenton-May, A.E.; Johnson, L.A.; Jackson, D.G.; Watson, S.P.; O'Callaghan, C.A. Renal cells activate the platelet receptor CLEC-2 through podoplanin. *Biochem. J.* **2008**, *411*, 133–140.
17. O'Callaghan, C.A.; Jones, E.Y. Structural and energetic aspects of multispecific immune recognition by NKG2D. *Structure (Camb.)* **2003**, *11*, 360–361.
18. Cueni, L.N.; Chen, L.; Zhang, H.; Marino, D.; Huggenberger, R.; Alitalo, A.; Bianchi, R.; Detmar, M. Podoplanin-fc reduces lymphatic vessel formation *in vitro* and *in vivo* and causes disseminated intravascular coagulation when transgenically expressed in the skin. *Blood* **2010**, *116*, 4376–4384.
19. Suzuki-Inoue, K.; Kato, Y.; Inoue, O.; Kaneko, M.K.; Mishima, K.; Yatomi, Y.; Narimatsu, H.; Ozaki, Y. Involvement of the snake toxin receptor CLEC-2 in podoplanin-mediated platelet activation by cancer cells. *J. Biol. Chem.* **2007**, *282*, 25993–26001.
20. Martin-Villar, E.; Scholl, F.G.; Gamallo, C.; Yurrita, M.M.; Munoz-Guerra, M.; Cruces, J.; Quintanilla, M. Characterization of human pa2.26 antigen (t1alpha-2, podoplanin), a small membrane mucin induced in oral squamous cell carcinomas. *Int. J. Cancer* **2005**, *113*, 899–910.
21. Uhrin, P.; Zaujec, J.; Breuss, J.M.; Olcaydu, D.; Chrenek, P.; Stockinger, H.; Fuertbauer, E.; Moser, M.; Haiko, P.; Fassler, R.; *et al.* Novel function for blood platelets and podoplanin in developmental separation of blood and lymphatic circulation. *Blood* **2010**, *115*, 3997–4005.

22. Schacht, V.; Ramirez, M.I.; Hong, Y.K.; Hirakawa, S.; Feng, D.; Harvey, N.; Williams, M.; Dvorak, A.M.; Dvorak, H.F.; Oliver, G.; *et al.* T1alpha/podoplanin deficiency disrupts normal lymphatic vasculature formation and causes lymphedema. *EMBO J.* **2003**, *22*, 3546–3556.
23. Mahtab, E.A.; Vicente-Steijn, R.; Hahurij, N.D.; Jongbloed, M.R.; Wisse, L.J.; DeRuiter, M.C.; Uhrin, P.; Zaujec, J.; Binder, B.R.; Schalij, M.J.; *et al.* Podoplanin deficient mice show a rhoa-related hypoplasia of the sinus venosus myocardium including the sinoatrial node. *Dev. Dyn.* **2009**, *238*, 183–193.
24. Douglas, Y.L.; Mahtab, E.A.; Jongbloed, M.R.; Uhrin, P.; Zaujec, J.; Binder, B.R.; Schalij, M.J.; Poelmann, R.E.; Deruiter, M.C.; Gittenberger-de Groot, A.C. Pulmonary vein, dorsal atrial wall and atrial septum abnormalities in podoplanin knockout mice with disturbed posterior heart field contribution. *Pediatr. Res.* **2009**, *65*, 27–32.
25. Hughes, C.E.; Navarro-Núñez, L.; Finney, B.A.; Mourão-Sá, D.; Pollitt, A.Y.; Watson, S.P. CLEC-2 is not required for platelet aggregation at arteriolar shear. *J. Thromb. Haemost.* **2010**, *8*, 2328–2332.
26. Tang, T.; Li, L.; Tang, J.; Li, Y.; Lin, W.Y.; Martin, F.; Grant, D.; Solloway, M.; Parker, L.; Ye, W.; *et al.* A mouse knockout library for secreted and transmembrane proteins. *Nat. Biotechnol.* **2010**, *28*, 749–755.
27. Bertozzi, C.C.; Schmaier, A.A.; Mericko, P.; Hess, P.R.; Zou, Z.; Chen, M.; Chen, C.Y.; Xu, B.; Lu, M.M.; Zhou, D.; *et al.* Platelets regulate lymphatic vascular development through CLEC-2-SLP-76 signaling. *Blood* **2010**, *116*, 661–670.
28. Suzuki-Inoue, K.; Inoue, O.; Ding, G.; Nishimura, S.; Hokamura, K.; Eto, K.; Kashiwagi, H.; Tomiyama, Y.; Yatomi, Y.; Umemura, K.; *et al.* Essential *in vivo* roles of the C-type lectin receptor CLEC-2: Embryonic/neonatal lethality of CLEC-2-deficient mice by blood/lymphatic misconnections and impaired thrombus formation of CLEC-2-deficient platelets. *J. Biol. Chem.* **2010**, *285*, 24494–24507.
29. Chippaux, J.P. Snake-bites: Appraisal of the global situation. *Bull. WHO* **1998**, *76*, 515–524.
30. Watson, A.A.; Brown, J.; Harlos, K.; Eble, J.A.; Walter, T.S.; O'Callaghan, C.A. The crystal structure and mutational binding analysis of the extracellular domain of the platelet-activating receptor CLEC-2. *J. Biol. Chem.* **2007**, *282*, 3165–3172.
31. Watson, A.A.; O'Callaghan, C.A. Crystallization and X-ray diffraction analysis of human CLEC-2. *Acta Crystallogr. Sect. F Struct. Biol. Cryst. Commun.* **2005**, *61*, 1094–1096.
32. Watson, A.A.; Christou, C.M.; James, J.R.; Fenton-May, A.E.; Moncayo, G.E.; Mistry, A.R.; Davis, S.J.; Gilbert, R.J.; Chakera, A.; O'Callaghan, C.A. The platelet receptor CLEC-2 is active as a dimer. *Biochemistry* **2009**, *48*, 10988–10996.
33. Watson, A.A.; Eble, J.A.; O'Callaghan, C.A. Crystal structure of rhodocytin, a ligand for the platelet-activating receptor CLEC-2. *Protein Sci.* **2008**, *17*, 1611–1616.
34. Hughes, C.E.; Pollitt, A.Y.; Mori, J.; Eble, J.A.; Tomlinson, M.G.; Hartwig, J.H.; O'Callaghan, C.A.; Futterer, K.; Watson, S.P. CLEC-2 activates Syk through dimerization. *Blood* **2010**, *115*, 2947–2955.
35. Krissinel, E.; Henrick, K. Inference of macromolecular assemblies from crystalline state. *J. Mol. Biol.* **2007**, *372*, 774–797.

36. Barrett, C.P.; Hall, B.A.; Noble, M.E. Dynamite: A simple way to gain insight into protein motions. *Acta Crystallogr. D Biol. Crystallogr.* **2004**, *60*, 2280–2287.
37. De Groot, B.L.; van Aalten, D.M.; Scheek, R.M.; Amadei, A.; Vriend, G.; Berendsen, H.J. Prediction of protein conformational freedom from distance constraints. *Proteins* **1997**, *29*, 240–251.
38. Humphrey, W.; Dalke, A.; Schulten, K. VMD: Visual molecular dynamics. *J. Mol. Graph.* **1996**, *14*, 33–38, 27–38.